SURFACE FUNCTIONALIZATION OF 1D LEPIDOCROCITE-LIKE TITANIA, AND CHARACTERIZATION OF 2D BIRNESSITE NANOMATERIALS

Rebecca R. Ramthun
In partial requirements for the
Degree of Bachelor of Science, B.S. in Chemistry
submitted to the Faculty of

WORCESTER POLYTECHNIC INSTITUTE
100 Institute Road
Worcester, Massachusetts 01609

CONTENTS

LIST OF FIGURES

PREFACE

Hydroxide-derived nanomaterials are a class of recently discovered semiconducting materials synthesized from manganese and titanium precursors to form 2D birnessite forms of MnO_2 and 1D lepidocrocite-like forms of TiO_2. Our objective is to understand the surface electronics of the Mn HDN for electrochemical, sensing, and catalytic purposes in the future, and to functionalize the surface of the 1DL for the purpose of incorporation into polymers. After synthesis, we utilized x-ray photoelectron spectroscopy (XPS) and powder x-ray diffraction (pXRD) to characterize the Mn HDN. Ultraviolet photoelectron spectroscopy (UPS) established a band edge diagram of the Mn HDN. Seeking to incorporate the 1DL into polymers in the future, we attached various silanes to the surface of the 1DL and confirmed attachment via XPS and XRD. Intercalated cation exclusion indicates confirmation of covalent attachment to the 1DL. Peak area ratios reveal that an aminopropyl silane attaches to the 1DL with a ratio of 0.98, and we present a model congruent with these results.

ACKNOWLEDGMENTS

GLOSSARY

HDN	Hydroxide-derived Nanomaterial
1DL	A one-dimensional lepidocrocite-like for of titania
TMB	TMAOH-derived birnessite
TiC	Titanium carbide
Anatase	A form of TiO_2 with a tetrogonal crystal structure
Birnessite	A form of MnO_2 in 2D sheets with cations intercalated inbetween for stability
TMA	Tetramethylammonium (1+ cation)
TMAOH	Tetramethylammonium hydroxide
UPS	Ultraviolet Photoelectron Spectra/Spectroscopy
XPS	X-ray Photoelectron Spectra/Spectroscopy
XRD	X-ray Diffraction
AFM	Atomic Force Microscopy

CHAPTER 1

INTRODUCTION TO HYDROXIDE-DERIVED NANOMATERIALS

Research and development worldwide has become increasingly focused on greener energy solutions, making the demand for accessible and inexpensive nanomaterials highly desirable. Badr and coworkers recently demonstrated a simple procedure for the development of 1D and 2D nanomaterials in a scalable, low-cost method using both manganese and titanium precursors that yield highly quantum confined materials.[1,2] Understanding the surface chemistry and interfacial electronics of these hydroxide-derived nanomaterials (HDNs) is incredibly desirable, as they have applications in solar cell catalysis, supercapacitors, batteries, chemical warfare agent protection, and more.[1,2] Mn and Ti HDNs were synthesized and characterized utilizing a variety of techniques. Because the titanium version of HDN generally follows a 1D lepidocrocite-based structure, we also refer to the Ti-based HDN as "1DL". In order to incorporate of the 1DL into polymers, we developed a procedure to attach a monolayer of silane to the titanium carbide based HDNs based off of our group's procedure to attach silanes to MXenes. We determined via XPS, UPS, and XRD that we had successfully produced Mn-based HDN that was consistent with the original material produced by Badr and coworkers. XPS

on the silane derivatized Ti HDN indicated successful covalent attachment before and after lithium chloride rinsing. The UP spectrum of the material is unique and has yet unknown implications; the work function after silane derivatization is drastically different from that of its precursor. Most critically, XRD of the material before and after derivatization indicates that the HDN is not destroyed by our current procedure and indicates surface attachment to the 1-D ribbons of 1DL. The results of this work provide a way forward for future researchers to use the silanes as a covalent "anchor" through which they can be incorporated into polymers.

CHAPTER 2

BACKGROUND

2.1 Introduction to HDNs

HDNs are a newly discovered class of nanomaterials that are synthesized via a reaction between a transition metal precursor and tetramethyl ammonium hydroxide. They were first produced in 2019 by a group of researchers at Drexel University in the hopes of forming 2D semiconducting materials without HF etching.[1]

In this reaction, the TMAOH is believed to act as both the solvent and the templating agent, producing a high yield of metal oxides with 1D and 2D configurations and quantum confinement.[3]

These emerging nanomaterials are incredibly desirable because of their unique surface chemistry and optoelectronic characteristics. HDNs are unique forsm of TiO_2 and MnO_2 semiconductors that are oxidatively stable, scalable, cost-efficient, and safer to make.

In addition, HDNs are good candidates for surface derivatization for the purpose of incorporation into polymers. Their work functions can be tuned by
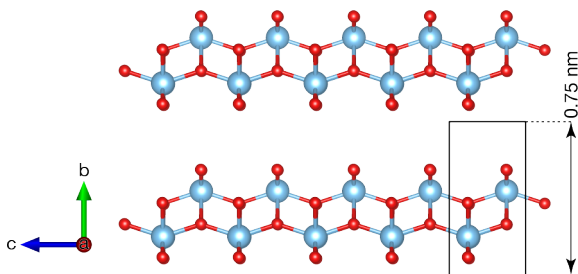
Figure 2.1. One-dimenional lepidocrocite-like TiO$_2$, 1DL. Adapted from Colin-Ulloa *et al.*, 10.1021/acs.jpcc.2c06719

the cation intercalated in between the atomic-level structures, as well as, we suggest, by cross-linkage-forming molecules such as functionalized silanes.[4] Such molecules could be used to manipulate the surface chemistry of these materials for a variety of purposes. This paper will discuss two kinds of hydroxide-derived nanomaterials: those derived from titanium, and those derived from manganese. Both materials utilize tetramethyl ammonium hydroxide, TMAOH, as a templating agent and exhibit self-assembling properties. Herein, we discuss the unique properties of each type, as well as a brief overview of silane chemistry, and how both shaped the overarching research objectives of this project.

2.2 Titanium HDN (1DL) Properties

The 1DL filaments, when formed in their one-pot synthesis, self-assemble into a variety of different kinds of nanomaterials,[3] but films of the material are amorphous and structures vary.[5] There is evidence that the 2D flakes as well as bundles produced in the material are the result of aggregated 1D filaments.[5] The 1DLs form quantum-confined one-dimensional structures that best resemble that of lepidocrocite. Our crystal model below shows the characteristic shape of the 1DL, with its interfacial Ti groups that present on either side in a zig-zag. Although similar to anatase, this form is distinct and does not possess its octahedral symmetry.[5,6] 1DL was previously ascribed an anatase-like shape, but more recent investigations have provided overwhelming support for the arrangement of the model shown in Fig 2.1.[5]

1DLs have been produced from precursors such as titanium carbides, silicides, and borides, and all present conversion as long as the titanium was not in its highest oxidation state.[1] This project will focus solely on the TiC-derived material, and it can be assumed that all data shown here is reflective only of 1DL with a carbide based precursor.

2.3 Mn-based HDN Properties

Manganese HDNs are 2–D, birnessite-based, manganese oxide materials that are derived from the reaction of Mn precursors such as Mn_3O_4, Mn_2O_3, MnB, etc.[2] They are also referred to as TMB, or tetramethylammonium-derived birnessite. For the purpose of this report, we refer to them as Mn HDN. As with the 1DLs, the TMAOH is the solvent and templating agent, both dissolving the manganese precursor and establishing the direction in which the complex will form. Birnessite nanosheets are highly desirable in the areas of photocatalysis and electrochemistry because of their high surface area.[7] Mn HDNs are easier to obtain than other methods to acquire Mn nanosheets, which are often multistep, high temperature, and laborious.[7] Mn HDNs are reported to have ~200 nm lateral sizes and highly ordered flakes of 2D hexagonal birnessite.[2] Although its initial discovery provided insight into its electrochemistry and optoelectronic properties, not enough is currently known about its valence electronics, it does not yet have an established band edge diagram, and the work function of the material is not yet known.

2.4 Silanes

Silanes are a class of compounds made of silicon and hydrogen. Silane based SAMs, or self-assembling monolayers, can be utilized to manipulate the surface chemistry of many compounds. The self-assembly of silanes happens due to the formation of polysiloxane, a polymer of silicon and oxygen atoms, which causes a grouping via Si–O–Si bonds.[8] This makes silanes manipulable covalent handles that can be attached to surfaces with presenting hydroxyls.[8]

Silanes present unique challenges; the presence of water triggers multilayer formation and polymerization of the silane with itself. To achieve monolayer coverage, water in the experiments must be removed or restricted.[8]

Another benefit of working with silanes is their effect on the electronics of materials. By introducing silanes with electron withdrawing or donating groups, they can inflict a dipole on semiconducting materials.[9] This effect on titania and Mxenes has been explored by our group previously.[10] The ribbons of amorphous HDN present a unique challenge, as their exact surfaces and surface chemistry are still not entirely known. Silanes are then a good tool for testing our model and learning more about how we can manipulate HDN surface electronics. Our model proposes TiO^- groups on both of its faces that would be readily accessible to the silanes, and it could theoretically bind three silanes to the surface of the material. This would additionally provide the benefit of greater control over the semiconductor's band gap as a function of the R group of the silane used.

Figure 2.2 demonstrates the dipole inflicted on the material as a result of the silane applied to the surface, wherein the silane with electron donating
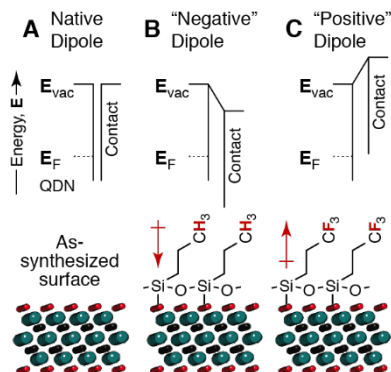
Figure 2.2. Surface dipoles on HDN as a function of the electron withdrawing or donating behavior of the silane attached to its surface. Adapted from Ref. 10.

groups ($-NH_3$) inflicts a negative dipole and the silane with the electron withdrawing groups ($-CF_3$) inflicts a positive dipole. Using the foundation of silane derivatization performed previously by A. Carl, J. Martin, and M. Frasch, we are now in a position to utilize silanization as a tool to better understand HDN surface chemistry. Through this project, we seek to synthesize and characterize 1DL and Mn HDN. We will develop a consistent and reliable method through which to attach silanes to the 1DL surfaces, and utilize this as tool to elucidate more electronic and structural properties of both materials.

CHAPTER 3

EXPERIMENTAL METHODS

3.1 Materials and Chemicals

3.1.1 HDN Synthesis Materials and Chemicals

All chemicals were used a received unless otherwise noted. The chemicals used to synthesize 1DLs included titanium carbide (99%, Strem Chemicals), tetramethylammonium hydroxide (25%, aq, ACROS Organics). For the manganese HDNs, the titanium precursor was replaced with manganese (II, III) oxide (Strem Chemicals). HDN synthesis was performed in 60 mL plastic reagent bottles (United Scientific) with 15 mm cross stir bars. Workup chemicals included ethanol (200 proof, Pharmco), lithium chloride (99+ %, Acros Organics), deionized water, and methanol (UV Grade, PharmCo), and workup was performed in 15 and 50 mL centrifuge tubes (ChemGlass Life Sciences).

3.1.2   Silane Materials and Chemicals

Silane solutions were prepared in piranha- and base-bath-cleaned glass dram vials. Chemicals utilized for silanization included (3-chloropropyl)trichlorosilane (TCI, >97%), (3-chloropropyl)triethoxysilane (TCI, >97%), 3-aminopropyltrimethoxysilane (Acros Organics, 95%), dry toluene, acetic acid (Fisher Chemical), ethanol, and methanol. Dried toluene was stored with activated molecular sieves (3Å, 1–2 mm beads, Alfa Aesar). Preparation of silanes occurred within a nitrogen recirculating flush box (Twin Glovebox, Terra Universal). Silanes attached to Ti-based 1DL after ethanol rinsing were transferred from their preparation vial to the reaction vial via 5 mL syringe (Fisher-Brand) and a $1\frac{1}{2}$"-long, 22-gauge needle tip. Argon gas (ultrahigh purity, Airgas) was bubbled through solution during the reaction via syringe and needle tip inserted through a rubber septum (Chemglass). Silanes attached to HDN after lithium chloride rinsing were stirred utilizing 10mm stir bars on a magnetic stirring hotplate located within the flushbox (Fristaden Lab).

3.1.3   Film making materials

All films for photoelectron spectra were airbrushed (Master Airbrush, model G233), onto a wafers of n^+-type-doped Si (111) silicon substrate (Addison Engineering). Substrates were heated to 90–130 °C on an aluminum-foil covered hotplate and secured with tweezers. Samples were sonicated utilizing a Branson 2510 sonicator.

3.1.4   Substrate Cleaning

Silicon substrates and glass dram vials were cleaned and prepared for all experiments utilizing a piranha solution of 3:1 concentrated sulfuric acid (H_2SO_4, 98%, Fisher Chemical) to aqueous hydrogen peroxide ($H_2O_{2(aq)}$, 30 wt %, Fisher). Caution: Piranha is a strong acid, strong oxidant, and it reacts extremely exothermically with organic matter.

3.2   Synthesis and Workup of HDNs

3.2.1   Initial Synthesis

For 1DLs, 1.0 g of TiC and 10.3 g of TMAOH were combined in a 60 mL plastic bottle with a $\frac{1}{16}$"-diameter hole drilled in the cap, with a 15 mm cross stir bar were placed in a oil bath stirring at maximum set to 50 or 85 degrees for 3-5 days. For manganese-based HDNs, the precursor was instead 1.0 g of Mn_3O_4.

3.2.2 Ethanol rinses

After heating, the material formed a thick black or dark brown "mud", which was then worked up in three phases. The product was first transferred to a 50 mL centrifuge tube via scraping with spatula and ethanol rinse as needed, with a total of 20 mL of ethanol added to the centrifuge tube. The tube was then vortexed for 30 s and centrifuged at 3900 rpm ($3000g$) for 5 min. After the first centrifugation, a supernatant of pale brown or yellow ethanol remained at the top. The color of the ethanol was recorded and discarded. 15 mL of ethanol was added, and the sample again vortexed, and centrifuged at 3900 rpm for 2 minutes. This step was repeated four times in total, with the supernatant discarded each time, and becoming increasingly clearer with each rinse. From here, the ethanol washed sample was either derivatized or characterized directly, or it proceeded to the next phase of work-up.

3.2.3 Water rinses

The second phase of work-up was the water rinse. The remaining, spun-down pellet after the ethanol wash had 20 mL of water added to it, and then it was vortexed to break up the pellet until a colloid is formed. Then it was centrifuged at ($3000g$) for 10 minutes. After the centrifuging, the liquid was poured into a fresh 50 mL centrifuge tube and the pellet tube labeled as such and stored or discarded. This was repeated once or twice, depending on the experiment. XP spectra indicated larger carbide peaks in the second water rinse, so for the most part, the first water rinse was used for LiCl washing and subsequent derivatization.

3.2.4 Lithium chloride rinses

The third phase was lithium chloride rinsing. Lithium chloride solution of 0.1 M in methanol or water was always made fresh prior to rinsing. First, 5 mL of HDN water colloid and 10 mL of 0.1 M LiCl solution were added to a 15 mL centrifuge tube and sonicated for half an hour, and then centrifuged at 3900 rpm for 2 minutes, the supernatant discarded. 10 mL of ethanol was then added to the HDN, the solution was vortexed, and centrifuged again with the same conditions. These ethanol rinses were repeated five times total. The final product was then either dried or kept in a sealed centrifuge tube until derivatized or characterized.

3.3 1DL Silane Attachment

3.3.1 1DL (Ethanol only) + Silane

Generally, the silane attachment on the ethanol-only rinsed HDN was performed with a 2:1 silane-to-1DL ratio by mass. For more information, consult
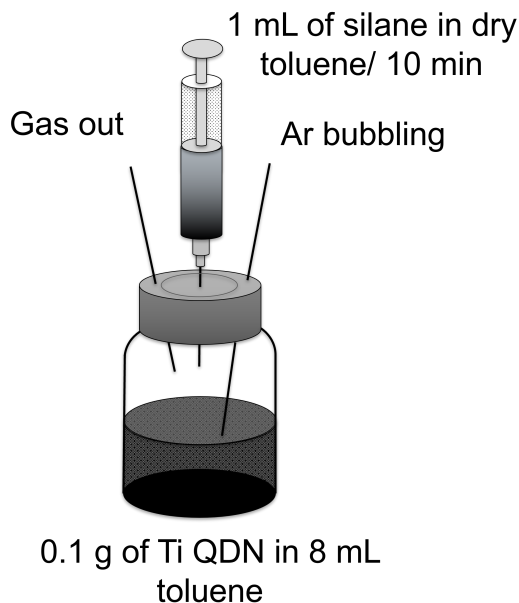
Figure 3.1. Graphic of the setup for the introduction of silanes to the 1DL solution. Gas out and the Ar (g) bubbling in solution represent needles poking through the septa top.

Appendix B. Silane aliquots were mixed in 5 mL of dry toluene in a 5D dram vial that was prepared in the flushbox. Meanwhile, ~0.1 g of ethanol washed HDN was dissolved in 8 mL of toluene in another dram vial and sonicated. A rubber septum was secured to the top of this glass dram vial and two needle tips were configured as in Figure 3.2 to create a flow of Ar gas bubbling through the solution. The silane solution was transferred out of the flushbox and into a 5 mL syringe, and 1 mL of the solution was added via syringe every ten minutes, the syringe remaining embedded in the septa to limit loss of silane. After all of the silane had been added, the septa and needles were removed and the solution was capped and a stirbar added. The solution was then stirred for two hours. The HDN & silane solution then underwent a rinsing procedure similar to that of the ethanol washes at the beginning, with the first rinsing being solely a centrifugation separate out a toluene suprenant, and the rest with ethanol added.

3.3.2   1DL (Lithium chloride in methanol) + Silane

Silane attachment after the 1DL had been lithium chloride rinsed was performed with a 1:10 silane to 1DL ratio. 109 ul of aminopropyltrimethoxysilane

in 5 mL of dry toluene in a 5D dram vial was prepared in the nitrogen recirculating flushbox. 0.5 g of 1DL in 7 mL of dry toluene were prepared under ambient conditions in a plastic centrifuge tube that was then vortexed and sonicated. 1 mL of 0.001 M acetic acid in ethanol was added to the tube and it was sonicated for five minutes.

The 1DL solution was pumped into the flushbox, and then the solution of 1DL in toluene and a 10mm stirbar was placed on the hotplate within the flushbox to maximum stirring. The silane solution was introduced slowly, and then the solution was covered with the dram vial's cap not fully tightened, and left stirring for an hour and a half.

After time, the dram vial was removed from the flushbox and immediately transferred to a plastic centrifuge tube and centrifuged for two minutes at ($3000g$) rpm. The dram vial was rinsed with ethanol and recapped, and sonicated while the centrifuge tube was centrifuged to remove residual materials. When the tube returned from centrifugation, the suprenant of mostly toluene was decanted and the ethanol solution used to rinse the dram vial was poured into the centrifuge tube. Another ethanol rinse and sonication was applied to the dram vial, and more ethanol, vortexing, and centrifuging was applied to the 1DL-silane mixture. This was repeated for a total of five times, with as much material removed as possible from the dram vial, and the ethanol suprenant being discarded until the final rinse, where it remained to keep the 1DL and silane material from drying out into flakes that were more challenging to work with.

3.4   Thin Film Deposition

Nitrogen-flow airbrush deposition was the preferred method used to prepare films of samples for photoelectron spectroscopy. The substrate was n+ silicon wafers that had been cleaned via RCA–1 and Piranha. Material to be airbrushed was prepared in plastic centrifuge tubes to the desired concentration, vortexed to disperse the settled material, and then sonicated constantly until it was pipetted into the airbrush's cup. The airbrush was situation 10 cm above an aluminum-foil covered hotplate set to 130 °C, with the substrate secured via metal tweezers. Pulses of the solution were applied in intervals dependent on visible drying speed of the solution on the surface of the substrate and were continued until after the film was visually uniform and the substrate was no longer visible. For explanations of the film-making process for other forms of analysis not discussed here, please consult Appendix C.

3.5   Photoelectron spectroscopy

A PHI5600 multitechnique system was used to acquire all x-ray and ultraviolet photoelectron spectra with a RBD instruments third-party acquisition
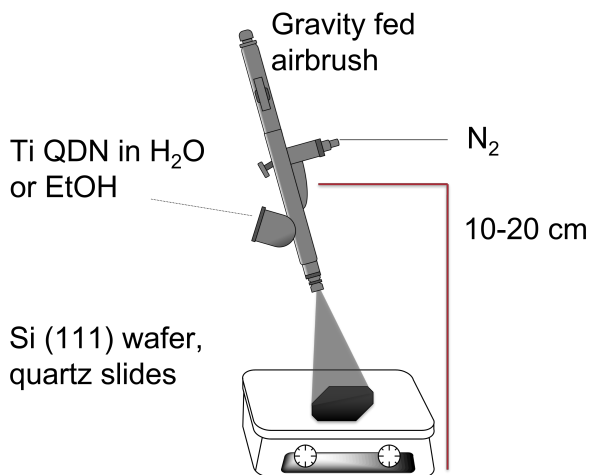
Figure 3.2. Diagram of the general airbrushing setup. Airbrush was secured by a ring stand with a clamp to allow for height adjustment.

system.[4] All surface state studies utilized monochromated Al Kα x-rays perpendicular to the detector.

XP collection for HDN samples did not utilize charge neutralization. The UHV pressures were $<1 \times 10^{-8}$ Torr and below for all acquisitions. After acquisition, all spectra were fit via a in-house-developed LabVIEW-based program. The He I spectroscopic line was produced by a helium gas discharge lamp (PREVAC, Poland, $h\nu$ = 21.218 eV), and He gas in the chamber was maintaind at ~15 mTorr. The power was set to 80 mA to maintain He I to He II radiation ratios. Instrumental calibration and UP spectra acquisition were performed by Julia L. Martin.[10]

3.6 pXRD

Samples for x-ray diffraction traces were spread via metal spatula onto the Teflon XRD plate and more material was added when ethanol-based 1DL or HDN dried in air into smaller pieces under ambient conditions. Flakes of sample were occasionally secured small slivers of carbon tape. The instrument was a Bruker-AXS D8 focus powder X-ray diffractometer, running on a 40 kV and 40 mA standard conditions.

CHAPTER 4

Mn HDN RESULTS

4.1 XPS

Figure 4.1 displays XP spectra of both the Mn HDN and its precursor, Mn(II, III) oxide. The Mn HDN sample whose spectra is presented here has been ethanol rinsed. The precursor peak positioning is consistent with literature.[11] The Mn 2p spectra in Figure 4.1A has prominent features at 643 and 654 eV, also consistent with literature for MnO_2, the latter being the $2p_{1/2}$ peak and the former being the $2p_{3/2}$ peak. At ~641 eV there is a shoulder that indicates unreacted Mn_3O_4.[2] The grey shaded peaks in N 1s and C 1s regions correspond with TMA^+ cations that are intercalated between the layers, keeping the birnessite sheets in place.

4.2 UPS

Figure 4.2 demonstrates the UP spectra of the same sample of ethanol rinsed manganese-based HDN as displayed in 4.1B, with two different fits, labeled as (A) Valence-band Case 1 and (B) Valence-band Case 2. The Fermi regions
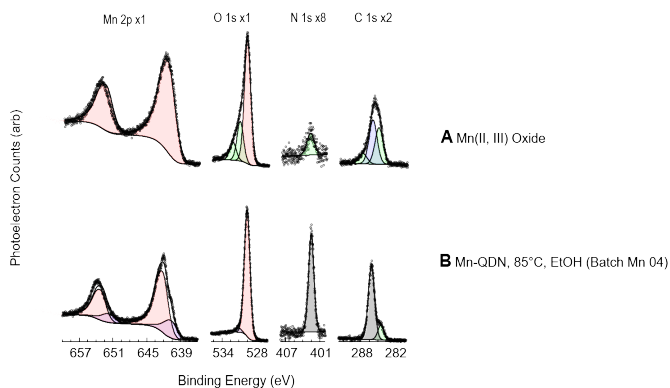
Figure 4.1. XP spectra of (A) birnessite material precursor, Mn(II, III) oxide, and (B) Mn HDN synthesized at 85°C, Ethanol rinsed. The red shaded regions indicate features retained from the precursor to the HDN, the purple regions indicate Mn HDN characteristics, the grey regions indicate TMAOH precursor, and the green regions indicate adventitious/unknown features.

are inset with a 10× multiplication factor. The red dashed line denotes the fit of the secondary electron cutoff energy, E_{SEC}, which intersects the x-axis at ~17 eV. The work function of this material is here calculated by the formula in eq 4.1.

$$\Phi = h\nu - E_{SEC} = E_{He\,I} - E_{He\,I} = 21.218 \text{ eV} - 17.113 \text{ eV} = 4.11 \text{ eV}. \qquad (4.1)$$

The green dashed line denotes the difference between the Fermi-level energy E_f and the valence-band maximum energy, E_{VBM}, which for Fit A is equal to 1.97 eV and for Fit B is equal to 0.87 eV. The indirect band gap, E_g, of the birnessite HDN material has been previously calculated to be 2.46 eV. Based on this band gap, $E_f - E_{VBM} = 1.97$ eV, and E_f and Φ of 4.11 eV, the calculations of the conduction band minimum E_{CBM} , for Fit A, is -3.63 eV vs E_{vac}. For Fit B, with a E_f - $E_{VBM} = 0.87$ eV fit instead, finds E_{CBM} = -2.52 eV vs E_{vac}.

4.3   pXRD

Figure 4.3 presents the XRD trace of ethanol-rinsed Mn HDN. We identify a (001) peak at 9.35°, a (002) peak at 18.85°, and a precursor trace (320) at 33.05°. Additionally, there is a wide, flat diffraction pattern throughout the entire scan ($2\theta = 0$–60°).
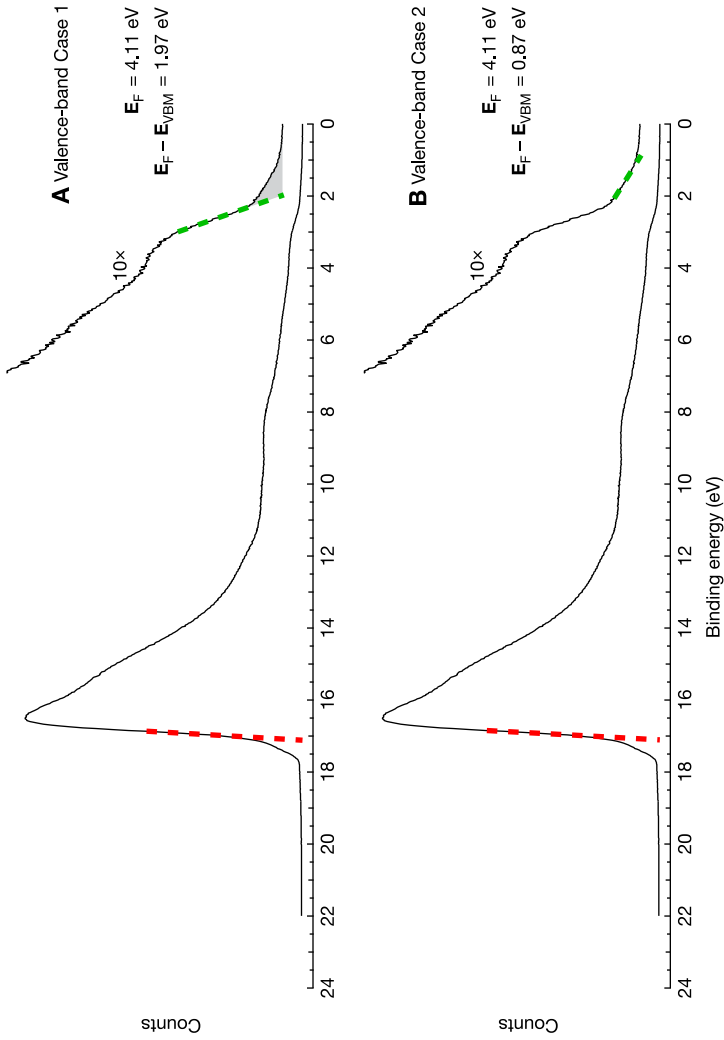
Figure 4.2. UP spectra of Mn HDN thin film (ethanol rinsed) on Si (111) substrate. The red dashed line fit denotes E_{SEC}, the secondary electron cutoff energy, and the green dashed fit denotes E_f - E_{VBM}
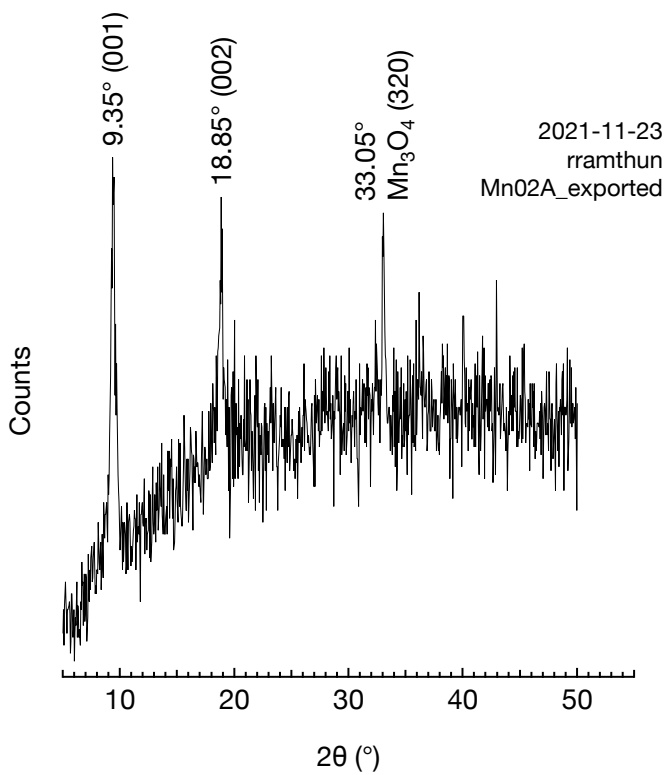
Figure 4.3. XRD Trace of the same sample of Mn HDN after ethanol rinsing.

CHAPTER 5

1DL RESULTS

5.1 Silane Attachment after Ethanol Rinsing

Figure 5.1 displays the XP spectra for Ti 1DL that has been ethanol washed only (A), ethanol-washed 1DL after its reaction with 3-chloropropyltrichloro-silane (B), and 1DL after its reaction with 3-chloropropyltriethoxy-silane (C). The red-shaded peaks for O 1s and Ti $2p_3$ we identify as the 1DL. We ascribe the features at ~455 eV and ~282 eV to unreacted titanium carbide precursor. As this material is not LiCl washed, there are still TMA$^+$ cations present; we ascribe the grey features to them (~404 eV N 1s, ~287 eV C 1s).

Figure 5.1B and 5.1C present features in the Si 2p and Cl 2p regions that are not present in Fig. 5.1A for the original material, a strong indication of silane on the surface of the material. Additionally, the peak positioning for the Cl 2p region is indicative of organic chlorine, which supports the idea is attached as part of an organosilane. There is a slight shift in the Ti $2p_{3/2}$ region for both materials after silane treatment from ~458 eV to ~459, potentially indicating charging on the surface as the result of multilayers of the silane.
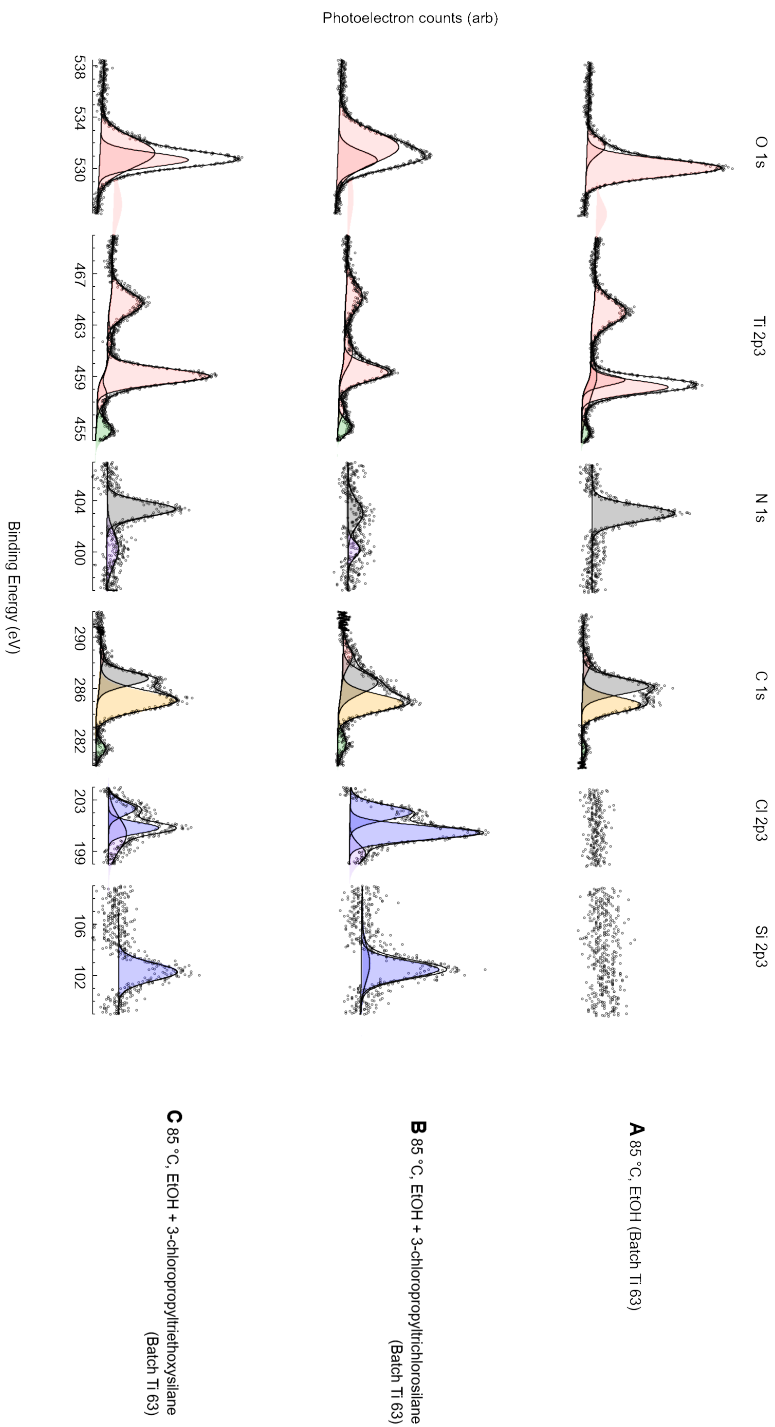
Figure 5.1. XP spectra of ethanol-rinsed Ti 1DL (A), with 3-chloropropyltrichlorosilane (B) and 3-chloropropyltriethoxysilane (C). Red-shaded features are 1DL-characteristic features. Blue features represent silane features. Pale green indicates unreacted titanium carbide precursor, and dark green represents chlorine cations. Yellow features are ascribed to adventitious species, and grey features represent unreacted TMA⁺ cations. The pale purple features represent unknown features.

5.2 Silane attachment after LiCl washing

Figure 5.2 above shows a comparison between the material before and after the addition of the silane (3-aminopropyl)trimethoxysilane (APTMS) to the solution. The blue shaded features are not present in Figure 5.2B, which displays the underivatized material, and we therefore conclude that the N 1s and Si 2p peaks in Fig. 5.2A can be attributed to covalently attached APTMS. Additionally, the N 1s feature (Fig. 5.2A) at ~399 eV is consistent with an amine group. The Si $2p_{3/2}$ peak's position, from 99 to 103 eV is consistent with the oxidized silicon in silanes and not with intrinsic silicon.

Of note is the resolution of the oxygen region, with a distinct separation in the peaks from Fig. 5.2A to 5.2B. The Ti region on Fig. 5.2A is smaller than that on Fig. 5.2B, but there is not a shift in peak positioning. Figure 5.2A also shows a much less intense Li 1s region, with much more noise than Fig.5.2B, making ascribing fits challenging.

All this in mind, this information cannot be used to incorporate the 1DL successfully if the silane attachment or its procedure breaks the material. Therefore, X-ray diffraction was implemented to confirm the integrity of the crystal structure of the 1DL after silane derivatization.

5.3 pXRD

Figure 5.3 presents the pXRD spectra of a lithium chloride rinsed sample of Ti 1DL before and after 3-aminopropyl)trimethoxysilane attachment. We ascribe a (001) peak at ~8° that matches 1DL literature for both samples[1]. We additionally identify precursor peaks at ~35 and 40°, and an overall amorphous characteristic to Fig.5.3A. Additionally, we note that the peak at 18° is an artifact of the Teflon scan plate.

5.4 UPS

Figures 5.4, 5.5, and 5.6 are the UP spectra for a selection of 1DL with various surface manipulations applied. Figure 5.4 displays the UP spectra of the material that still has TMA$^+$ intercalated and was derivatized with APTMS. Figure 5.5 is the UP spectra of 1DL that has been rinsed with LiCl, and Figure 5.6 is, likewise, a UP spectrum with 1DL that has had cation exchange performed and then APTMS derivatization. The Fermi regions are inset with a 20× multiplication factor.
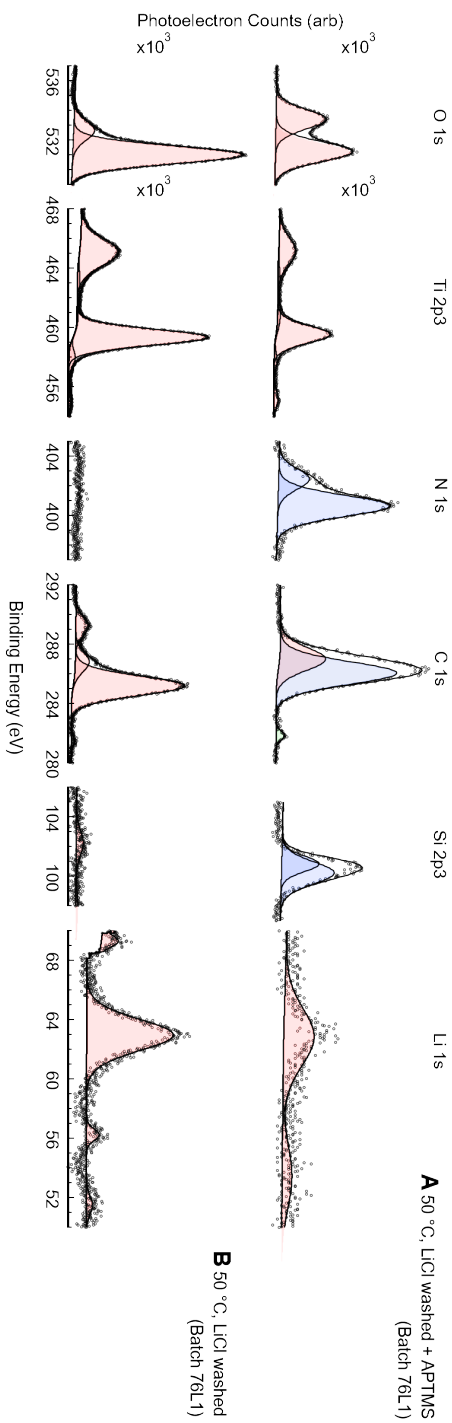
Figure 5.2. XP spectra of LiCl-washed Ti 1DL, with and without (3-aminopropyl)trimethoxysilane. The red fits represent 1DL and LiCl features, while the blue fits represent features ascribed to the silane.
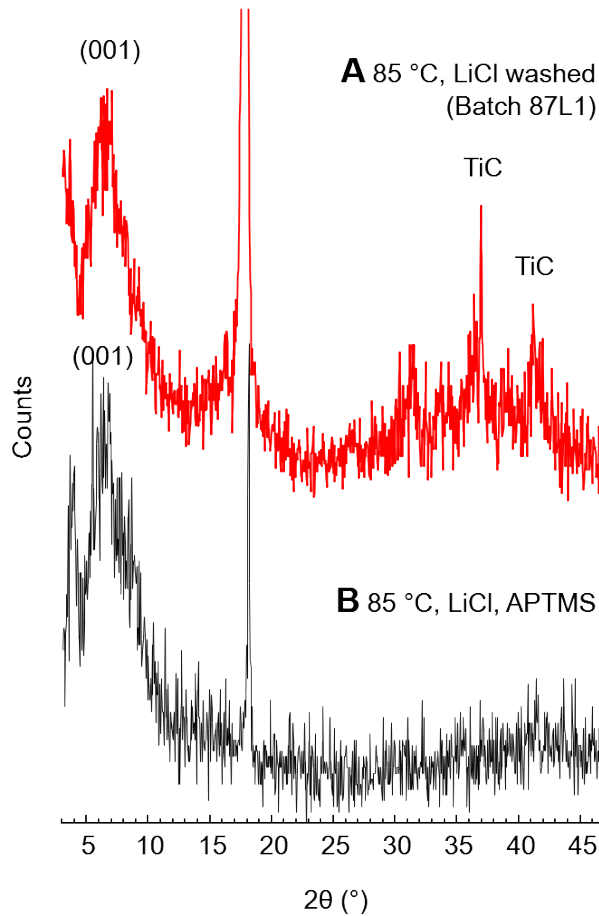
Figure 5.3. XRD Trace of LiCl rinsed 1DL before and after APTMS is attached to the surface of the material.

As with the Mn HDN UPS, the red dashed line denotes the secondary electron cutoff energy, E_{SEC}, and the green dashed line denotes the difference between the Fermi-evel energy, E_f, and the valence-band maxima, E_{VBM}. The work function was calculated by the formula in eq 5.1 where $E_{He\,I} \equiv 21.218$ eV.

$$\phi = h\nu - E_{SEC} = E_{He\,I} - E_{SEC} \tag{5.1}$$
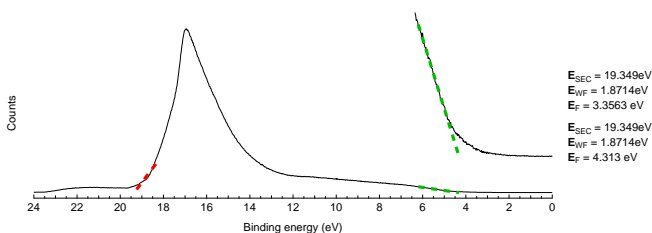
Figure 5.4.   UP spectra of 1DL (ethanol rinse only) with (3-aminopropyl)trimethoxysilane attached.
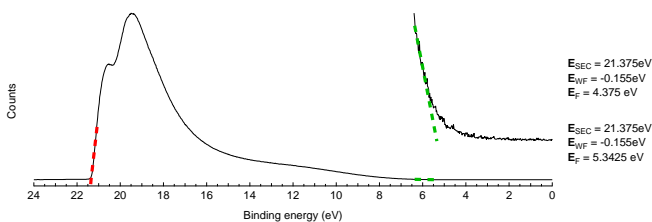
Figure 5.5. UP spectra of 1DL (LiCl rinsed).
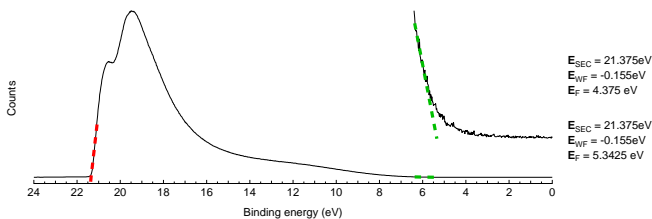
Figure 5.6. UP spectra of 1DL (LiCl rinsed) with (3-aminopropyl)trimethoxysilane attached.

Table 5.1. Electronic properties of 1DL with covalently attached APTMS and LiCl rinsing. All energy values, E, and work function values, ϕ, are in eV.

UP Spectrum	Conditions	E_{SEC}	ϕ	$E_f - E_{VBM}$
5.4	1DL (EtOH only) + APTMS	19.35	1.87	4.31
5.5	1DL (LiCl)	17.26	3.96	3.86
5.6	1DL (LiCl) + APTMS	21.38	-0.16	5.34

5.5 Peak Area Ratios

We calculated the peak area ratios of the N 1s and Ti 2p peaks for the APTMS derivatized 1DL sample (Batch 76L1 and APTMS) that was displayed in Fig.5.6. N and Ti were chosen because (3-aminopropyl)trimethoxysilane only possess one N group for every silane, and 1DL is a nanofilament composed of repeating TiO_2 units.

N to Ti ratios were calculated by adding all of the trapezoidal integrations of the multiplex fits presented in the peak-fitting program, dividing each by their respective sensitivity factor, and then dividing the N area by the Ti area to calculate the final results. The N 1s area was 1918 eV cps, and its sensitivity factor is 0.477. The Ti 2p had a raw area of 8201 eV cps with a sensitivity factor of 2.001. The resulting N to Ti ratio on the surface of the material was 0.98.

CHAPTER 6

DISCUSSION

6.1 Mn HDN Discussion

6.1.1 XPS

Our peak positioning for the Mn HDN is consistent with published data for Mn 2p and O 1s, and we additionally present the N and C regions to assert the presence of unreacted TMAOH. We affirm that we have correctly made tetramethylammonium derived birnessite and are in a position to discuss its electronic and crystal properties further.

6.1.2 pXRD

The published XRD peaks for Mn HDN (horizontal alignment) mark the (001) trace at ~9°, and their (002) peak at ~19°.

As seen in Figure 6.1, which displays a VESTA-calculated idealized diffraction trace for Mn HDN precursor, there are notable precursor peaks at 33°. Compared to our pXRD, Figure 4.3, we were able to first, confirm that we have
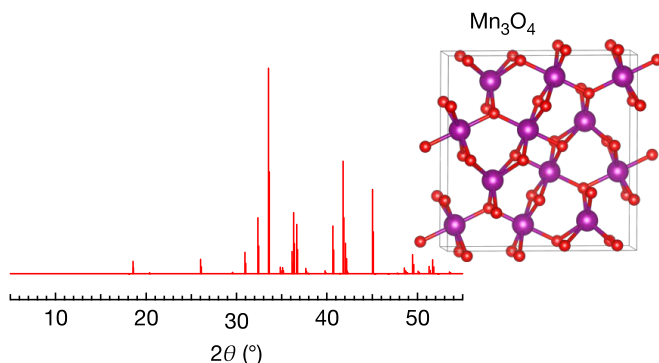
Figure 6.1. Idealized XRD trace for Mn_3O_4 and its accompanying atomic model.

the correct crystal structure of Mn HDN, and second, identify (as expected) unreacted precursor in a material that has not been water rinsed, the process of which usually removes the Mn-contributing precursor. We conclude that we have properly synthesized the right form of the Mn HDN.

6.1.3 UPS

The previously introduced fits for Fig. 4.2 put us in a position to, in conjunction with the previously calculated band gap of the Mn HDN material, construct a band edge diagram of this nanomaterial for the first time. The work function for this material as determined by UPS is ~4.03 eV. The combination Fermi edge and Tauc calculations for Case 1 establishes valence and conduction band edges at –6.09 eV and –3.63eV, while Case 2 establishes them at –4.98 eV and –2.52 eV. Based on this data, we construct a hypothesis for future electrochemical testing to verify the dopant type and intensity of this material.

Figure 6.2 indicates strong n-type doping, with a difference between the conduction band edge and the Fermi level of only ~0.5 eV. Figure 6.2B indicates mild p-type doping, with the Fermi level slightly closer to the valence band maxima than the conduction band minima.

This offers the ability to create hypothesis-driven experiments that can corroborate our band edge. From here, electrochemical experiments represent a viable way to test these parameters on an absolute thermodynamic scale.

A Case 1, $E_F - E_{VBM} = 1.97$ eV   **B** Case 2, $E_F - E_{VBM} = 0.87$ eV

Energy vs E_{vac} (eV)

Case 1 (A):
- $E_{CBM} = -3.63$ eV
- $E_F = -4.11$ eV
- $E_{VBM} = -6.09$ eV

Case 2 (B):
- $E_{CBM} = -2.52$ eV
- $E_F = -4.11$ eV
- $E_{VBM} = -4.98$ eV
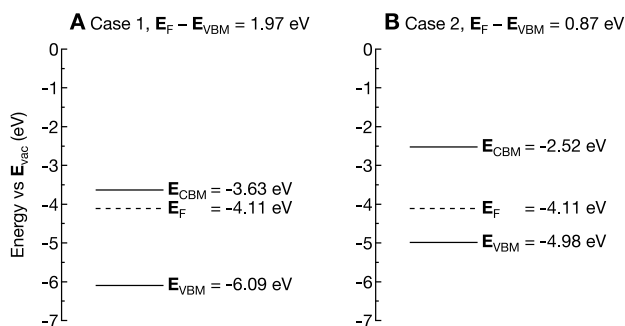
Figure 6.2. Band edge diagram of (A) Valence-band Case 1 and (B) Valence-band Case 2 fits of manganese-based HDN

6.2   1DL and Silane Discussion

6.2.1   Silane Derivatization Alters Work Function

The initial motivation behind attaching a silane to the surface of the HDN material was to apply a dipole to the surface and alter the band gap via the implementation of electron-withdrawing or donating groups, as well as to functionalize the material for better incorporation into polymers in the future. Firstly, we were able to attach silane to the material before and after the lithium chloride rinsing step. As previously demonstrated by our group, lithium chloride rinsed material usually displays a work function of 4.0 eV.[2] Julia Martin also recently demonstrated manipulation of the work function of MXenes via silane attachment[8], providing evidence that silanes could be used to "tune" band edges of low dimensional materials.

Our UP spectra and respective fits help assert that the work function is changing as a result of silane attachment to the 1DL surface. Figure 5.5, the UP spectra of LiCl-washed 1DL, has a work function close to those previously assigned to 1DL.[2] After the attachment of an electron-donating silane, APTMS, as seen in Fig. 5.6, the work function is less than that of Fig. 5.5, its precursor. This indicates that APTMS is inflicting a negative dipole on the surface.[9] The number itself (–0.16 eV) is uncommon for these materials, and requires further investigation before the implications can be understood.

6.2.2   Silane Derivatization Mechanism and Attachment

Although we have been able to elucidate much about the 1DL material since its discovery, we are still not certain what it looks like on a nanoscale level. We know that the material is not homogenous, and it could display a variety
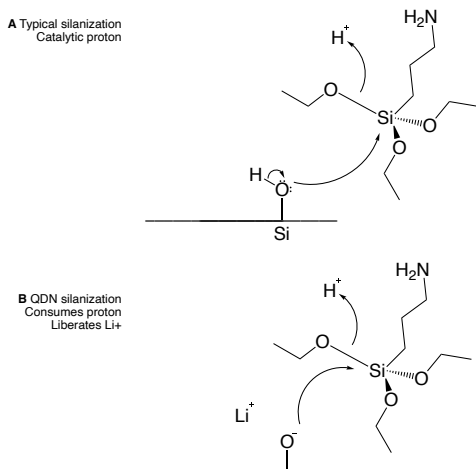
Figure 6.3. Mechanism of silane reaction onto surfaces.

of different behaviors as a result of the alignment of the 1DL nanofilaments. However, after performing silane derivatization, we may have a road map to identifying more critical aspects of the surface chemistry of this material. Based on the photoelectric spectra and peak ratios from our results, we present a theoretical model (Figure 6.3) that suggests the method of silane derivatization to the surface of 1DL.

Figure 5.1, which presents silane attachment to the material after only ethanol rinsing, displays a clear loss of TMA$^+$ ascribed features (grey) after the introduction of both silanes. Figure 5.2, which presents silane attachment to the material after lithium chloride cation exchange, displays a clear loss of Li ascribed features (grey) after the introduction of the silanes. We posit that the silanization reaction "kicks" out the intercalated cations when they bind to the silane, which is supported by the XP spectra. Figure 6.3A displays a standard silanization procedure on a Si substate with –OH surface groups, where the Si acts as a Lewis acid. Figure 6.2B demonstrates a model based on the XP spectra.

What is still unknown based on this model, is how many silanes bind to each Ti–O$^-$ termination point on our proposed 1DL model, which is where our peak area ratios may provide some clarity. Our calculation in §5.5 determined the N to Ti peak ratio of 0.98. A model consistent with this data would represent one APTMS silane attached at *every* titanium-oxygen site within a 1DL nanofilament, as opposed to one APTMS binding to multiple spots on the surface at once.

CHAPTER 7

CONCLUSIONS AND FUTURE WORK

7.1 Mn HDN

This project sought to synthesize and characterize the Mn HDN and expand our knowledge on its electronic properties. We successfully made the material and constructed a band-edge diagram for the material for the first time. Given this information, future researchers can utilize electrochemical experiments to inform both our understanding of its properties, and our understanding of how to prepare our UP fits on the material moving forward.

It would be incredibly valuable to our understanding of the Mn HDN to attach silanes to the surface of the birnessite material, much as was performed in this MQP on 1DL. The Mn HDN should be rinsed in LiCl suspended in methanol in order to remove as much water as possible prior to the introduction of the silane, and then the procedure could most likely be followed nearly identically to those already outlined in this paper. This information would guide our understanding of the interstitial dipoles that directly impact the electronic properties of this structure for any future applications.

7.2   1DL

Assessing the coverage of 1DL by silanes utilizing a substrate-overlayer model is the next strong theoretical step. Overlayer models help create an idealized model of a system where overlayer species attenuate, or reduce the counts of photoelectrons that can be released by the layers beneath[4]. This robust method would give us increased confidence in our understanding of how the silane attaches to the HDN.

We don't yet have clear AFM demonstrating characteristic morphology of an HDN with a silane attached to its surface. It would be ideal to be able to get AFM of Mn HDN and 1DL with silanes attached to it. AFM of the material, especially images that could capture aligned nanofilaments or sheets, and a comparison of material before and after surface derivatization would be incredibly useful to informing our modelling of the material and help us understand what the morphology of silane attached to HDN looks like.

Our collaborators have hypothesized that there is the potential for the HDNs to be fragile in acidic environments. The current procedure to attach silanes without very electronegative R-groups to the surface of the 1DL uses 0.1 M acetic acid in ethanol to "spike" the solution, pushing the reaction forward. Future researchers should note that as much water was removed from this procedure as possible to prevent the silane from polymerizing with itself and encourage the reaction with the 1DL surface. This in mind, it is possible that the presence of the acid could be converting the 1DL to an anatase analog instead of its current proposed lepidocrocite-like shape, or it could be breaking the 1D structure entirely. Raman spectroscopy is needed to determine if the introduction of acetic acid to the material during silane reactions is damaging the material.

Throughout the research on the titanium carbide-derived material by myself and the titanium boride-derived material by Julia Martin, multiple instances of gel formation occurred. The gelling of the titanium boride precursor material was initially ascribed to the behavior of boride polymers, but with the carbide precursor material also gelling, further investigation into both is certainly needed. More information and documentation on the gelling behavior can be found in Appendix D, where there are photos documenting the 1DL in a gel phase.

Within this report, we provide evidence that we have successfully attached multiple silanes to the 1DL, and are beginning to understand how they can be used to tune the surface electronics of the material. I would recommend that the next researcher with this material attach a CF_3 (electron-withdrawing) silane to the surface of the material and compare the band edge diagrams formed as a result of the shift in work functions. More investigation is also needed to better understand the work function of the APTMS silane on the surface of the lithium chloride rinsed 1DL.

We believe that the silane derivatization procedure established throughout the course of this project will provide a covalent handle through which 1DLs can be incorporated into polymers. With evidence that there is silane attachment, future researchers can now begin experimentation to incorporate or seal 1DL into new materials. Vinyl or allyl terminated silanes could be attached to the 1DL for the incorporation into natural latex for the purpose of designing better barriers for chemical warfare agent protection.

In conclusion, we synthesized and characterized 2D birnessite and functionalized the surface of 1D lepidocrocite-like titania. Characterization methods of the Mn HDN included x-ray photoelectron spectroscopy and x-ray powder diffraction. We then utilized ultraviolet photoelectron spectroscopy to form a band edge diagram for this novel material. The 1DL was derivatized after two steps in its workup, with successful silane attachment both times. We developed a model of silane attachment congruous with a calculate peak area ratio of 0.98 for an aminopropyl silane to the surface of 1DL.

APPENDIX A

REFERENCES

1. Badr, H. O.; El-Melegy, T.; Carey, M.; Natu, V.; Hassig, M. Q.; Johnson, C.; Qian, Q.; Li, C. Y.; Kushnir, K.; Colin-Ulloa, E.; et al. Bottom-up, scalable synthesis of anatase nanofilament-based two-dimensional titanium carbo-oxide flakes. *Materials Today* **2021**. 10.1016/j.mattod.2021.10.033.

2. Badr, H. O.; Montazeri, K.; El-Melegy, T.; Natu, V.; Carey, M.; Gawas, R.; Phan, P.; Qian, Q.; Li, C. Y.; Wiedwald, U.; et al. Scalable, Inexpensive, One Pot, Synthesis of Crystalline Two-dimensional Birnessite Flakes. *Matter* **2022**, *4* (7), 2365–2381. 10.1016/j.matt.2022.05.038

3. Colin-Ulloa, E.; Martin, J. L.; Hanna, R. J.; Frasch, M. H.; Ramthun, R. R.; Badr, H. O.; Uzarski, J. R.; Barsoum, M. W.; Grimm, R. L.; Titova, L. V. Electronic Structure of 1D Lepidocrocite TiO_2 as Revealed by Optical Absorption and Photoelectron Spectroscopy. *J. Phys. Chem. C* **2023**, *127* (15), 7275-7283. 10.1021/acs.jpcc.2c06719

4. Carl, A. D. Soft, Organic, Carrier-Selective Contacts at Inorganic Semiconductor Interfaces Enabled by Low-Defect Covalent Bonding. Ph.D. Dissertation, Worcester Polytechnic Institute, Worcester, MA, **2020**.

5. Badr, H. O.; Lagunas, F.; Autrey, D. E.; Cope, J.; Kono, T.; Torita, T.; Klie, R. F.; Hu, Y.-J.; Barsoum, M. W. On the structure of one-dimensional TiO_2 lepidocrocite. *Matter* **2023**, *6* (1), 128-141. 10.1016/j.matt.2022.10.015

6. Ma, J.; Reeves, K. G.; Porras Gutierrez, A.-G.; Body, M.; Legein, C.; Kakinuma, K.; Borkiewicz, O. J.; Chapman, K. W.; Groult, H.; Salanne, M.; *et al.* Layered Lepidocrocite Type Structure Isolated by Revisiting the Sol–Gel Chemistry of Anatase TiO_2: A New Anode Material for Batteries. *Chem. Mater.* **2017**, *29* (19), 8313-8324. 10.1021/acs.chemmater.7b02674

7. Kazuya Kai, Y. Y., Hiroshi Kageyama, Gunzi Saito, Tetsuo Ishigaki, Yu Furukawa, and Jun Kawamata. Room-Temperature Synthesis of Manganese Oxide Monosheets. *J. Am. Chem. Soc.* **2008**, *130* (47), 15938-15943, Room-Temperature Synthesis of Manganese Oxide Monosheets. 10.1021/ja804503f

8. Ulman, A. Formation and Structure of Self-Assembled Monolayers. *Chem. Rev.* **996**, *96* (4), 1533-1554. 10.1021/cr9502357

9. Gleason-Rohrer, D. C. Measurement of the Band Bending and Surface Dipole at Chemically Functionalized Si(111)/Vacuum Interfaces. *J. Phys. Chem. C* **2013**, *117*, 18031–18042. 10.1021/jp401585s

10. Martin, J. L. Surface Science of Low-Dimensional Materials. Ph. D. Dissertation, Worcester Polytechnic Institute, Worcester, Massachusetts, USA. **2023**.

11. Moses Ezhil Raj, A.; Victoria, S. G.; Jothy, V. B.; Ravidhas, C.; Wollschläger, J.; Suendorf, M.; Neumann, M.; Jayachandran, M.; Sanjeeviraja, C. XRD and XPS characterization of mixed valence Mn_3O_4 hausmannite thin films prepared by chemical spray pyrolysis technique. *Appl. Surf. Sci.* **2010**, *256* (9), 2920–2926. 10.1016/j.apsusc.2009.11.051

12. Carl, A. D.; Grimm, R. L. Covalent Attachment and Characterization of Perylene Monolayers on Si(111) and TiO_2 for Electron-Selective Carrier Transport. *Langmuir* **2019**, *35* (29), 9352–9363. 10.1021/acs.langmuir.9b00739

13. Frasch, M. H. A New 1-D Semiconductor for Sensors, and Functionalizing the MXene Surface. MQP (Undergraduate) Dissertation, Worcester Polytechnic Institute, Worcester, MA. **2022**.

APPENDIX B

NOTES ON DERIVITIZATION

Over the course of my time working with this project, I used several procedures in the attempt to get silane on the surface of the material. The purpose of this appendix is to lay out some of the pitfalls future researchers may encounter and my recommendations on future silane derivatization procedures. I have also listed all the silanizations I have performed and the ratios used.

B.1   Silane Attachment on a Si Wafer

This procedure was adapted from Alex Carl's TiO$_2$ and Si derivitization.[12]

Recommendation from MHF:

400 μL of aminopropyltriethoxysilane (APTES) and 10 mL of ethanol, stirred in the flushbox overnight.

Actual silane prep:

500 μL of (3-chloroproyl)triethoxysilane and 5 mL of toluene was prepared in a dram vial in the flushbox with stirring overnight.

Si wafer, n$^+$ SSP Si (111) RCA–1 cleaned in DI water, Ar gun dried. Si wafer was transferred into the flushbox and then sat in the silane solution for four hours. After the four hours, the silane solution was decanted and the wafer was sonicated for 10 min in 3 mL of toluene. It was then sonicated in 3 mL of methanol, and then for 10 minutes with 3 mL of water. It was then dried under Ar and stored in a petri dish.

B.2   JLM/MHF Procedure

Adapted from MHF & JLM procedure for silanizing MXenes.[10,13]

1. Silane prep: 279 μl of APTES, 5 mL of toluene prepared in the flushbox the day before silanization.

2. Degassed 2 mL of DI H_2O in a plastic test tube using the sonicator

3. Added 0.119 g of 1DL (Batch 58, ethanol rinsed only), and 5 mL of ethanol into a glass dram vial. Next, 2 mL of 0.1 M acetic acid were then added along with the degassed water.

4. The sample was then prepped in the same configuration as was previously detailed in Fig. 3.2. The prepared silane was removed from the flushbox and quickly loaded into a 5 mL syringe, which was directly inserted into the septa and remained there for the duration of silane loading into the solution.

5. Added 0.5 mL of silane to the solution every ten minutes. The solution reacted for 6 hours and then was rinsed with a standard 1DL ethanol wash sequence.

Lessons learned:

1. The silane in toluene solution does not need to be prepared the night before. The time it takes to set up the 1DL for the reaction is sufficient time.

2. The water in the procedure is unnecessary.

3. The reaction doesn't need 6 h.

B.3   More Derivitizations

B.3.1   Batch 60 & CF$_3$ Silane

1. Silane: (3,3,3-trifluoropropyl)trichlorosilane. 195 μL of CF$_3$-terminated silane in 5 mL of toluene prepped in the flushbox.

2. 0.1 g of 1DL, 8 mL of toluene prepped outside flushbox. Setup was identical to prior procedure, but Ar bubbling was stopped once all the silane was added. Reaction was run for 2.5 hrs.

B.3.2   Batch 62 & APTES

1. Tried using a plastic culture tube for the reaction and N_2 bubbling. Had issues with the septa sizing, would not recommend this adjustment.

B.3.3   Batch 63 Silanizations

Procedure followed as listed in the Experimental Methods chapter, Ch. 3. Consistently had issues with very small yields, needed to adjust amount of 1DL used.

B.3.4   Batch 69 (water-rinsed) silanization

The water washed colloid (Ti Batch 69) had so much water in that it immediately made a chunky polymer. Would not recommend unless thoroughly dried the colloid somehow. Additionally N_2 bubbling through the colloid thickened the solution.

B.3.5   Batch 69L1, 69L2 Silanization

Objective: Silane lithium chloride rinsed material.

1. ~0.1 g of 1DL, 1 mL of 0.1 acetic acid in ethanol, and 7 mL of dry toluene in a glass dram vial were sonicated for 20 minutes. N_2 was added to the solution in a similar fashion to the silane setup with septa to encourage the 1DL to dissolve in the toluene which was proving challenging.

2. After, the samples were setup in the septa-needle-configuration and APTMS silane was added, 1 mL every ten minutes. Then the septa was removed, the top secured, and a stir bar added. The samples were stirred on hotplates for 3 h and then worked up with ethanol.

Notes: The workups had to be halted because the pellets of material were incredibly small, too small to continue to feasibly "rinse".

Lessons learned:

1. <0.5 g of 1DL is insufficient for silane procedures.

2. The water in lithium chloride rinsing step is polymerizing the silane, making it challenging to get 1DL-silane interactions and a monolayer on the surface.

. . . which led to the lithium chloride rinse happening in methanol instead of water, which led to the procedure outlined in Ch. 3.

B.3.6 Recommendations

If TMA$^+$ intercalated between the layers is acceptable, silane reactions can happen after the ethanol workup. If Li$^+$ is preferred, use a LiCl solution in methanol to rinse the 1DL prior to silanization. Remove water from the reaction as much as possible, and limit silane exposure to air by performing all silane reactions in the N$_2$ flushbox with stirring. <0.5 g of 1DL is a good starting point to give you enough material to work with at the end of the synthesis.

To prevent charging of the material due to oversilanization (more than a monolayer) when working with APTMS and lithium chloride washed material, a 1:10 ration of silane to 1DL is recommended.

APPENDIX C

FILMMAKING

Films were made for a variety of purposes throughout the process of this experiment. The procedure for making films on silicon wafers was previously detailed in Ch. 3.

Films made on quartz for optoelectronics for our physics department collaborators were most commonly made with the water colloid diluted down 1:5 or 1:10. The hotplate could be set to 130 °C or higher, and around five to ten passes were sufficient.

Films made on FTO (fluorine-doped tin oxide glass) for electrochemistry were made with a 1 10 dilution of ethanol or lithium chloride rinsed 1DL sonicated up until airbrushing, and the material was airbrushed with enough passes to make a thick layer on the surface of the substrate. FTO was prepared by our collaborators within 24 hours of film deposition.

APPENDIX D

AFM IMAGING

When preparing 1DL or HDN films for AFM analysis, the films must be very, very dilute. 10 to 1 dilutions of 1DL in water or ethanol with five passes with the airbrush resulted in films that were still too thick. My personal recommendation is to dilute the solution to 1:100 with intense sonication prior to airbrushing, with five passes, and scale up from there as necessary. Before looking at the material under AFM, utilize the Keyence digital microscope in LEAP to get a better idea of the material coverage and if the sample is likely to display any areas with morphology that can be clearly photographed.

The images we did get are presented here. The sample is 1DL Batch 87L1 and APTMS, which was made at 85 °C and rinsed with LiCl in methanol. There is another image of 1DL Batch 87L1 without silane on its surface, which is included in the next appendix as evidence of the gel behavior of that sample. All AFM images were taken by Erika Colin-Ulloa.
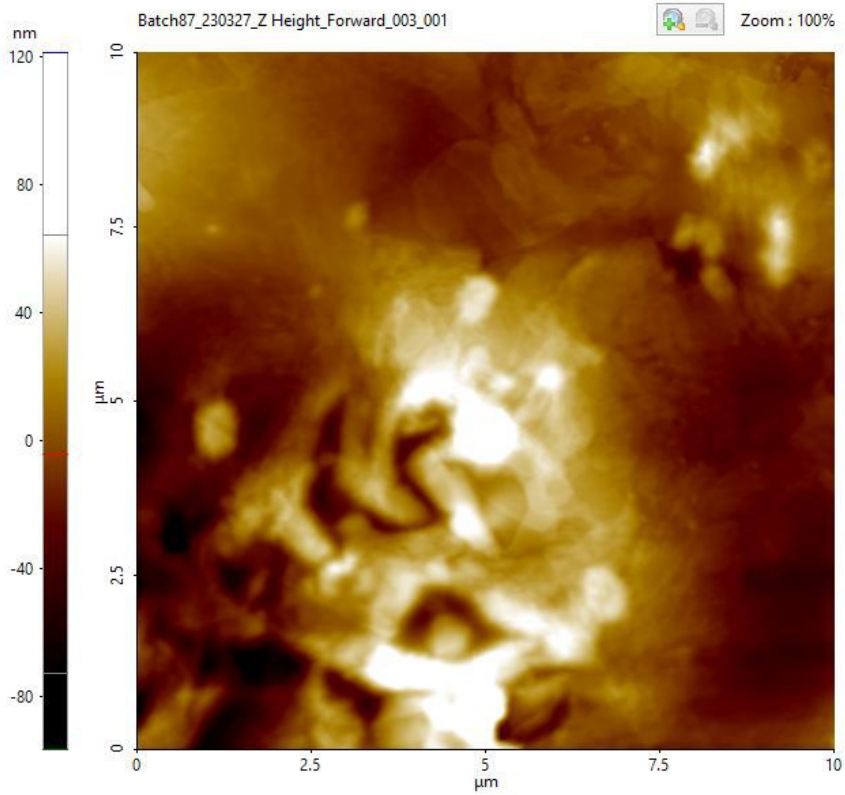
Figure D.1. AFM Image of lithium chloride washed 1DL Batch 87 with APTMS, first position
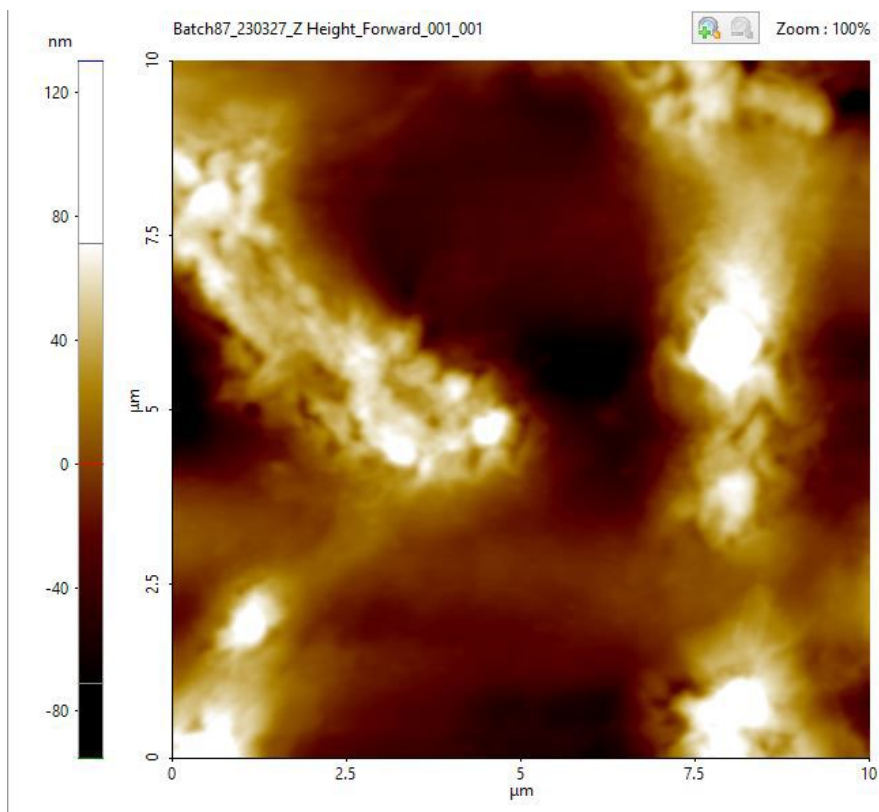
Figure D.2. AFM Image of lithium chloride washed 1DL Batch 87 with APTMS, second position

APPENDIX E

GEL BEHAVIOR OF TiC 1DL

Our lab has confronted challenges with the Titanium-based 1DL changing into a clear, gel-like form at a variety of different stages in its workup. Initially suspected to be a behavior occurring solely with the titanium boride-precursor materials, JLM first recorded evidence of this behavior occurring. However, I also encountered gelling behavior with materials with a TiC precursor, most commonly after lithium chloride washing. Below is evidence for it occurring with Batches 69 and 87, both high temperature runs that were lithium chloride washed. Batch 87L1's gelling was not visible until prepared for AFM, at which point small gel droplets could be seen on its quartz slide, and then were very apparent under AFM, which caused the blurring seen in Fig E.3.
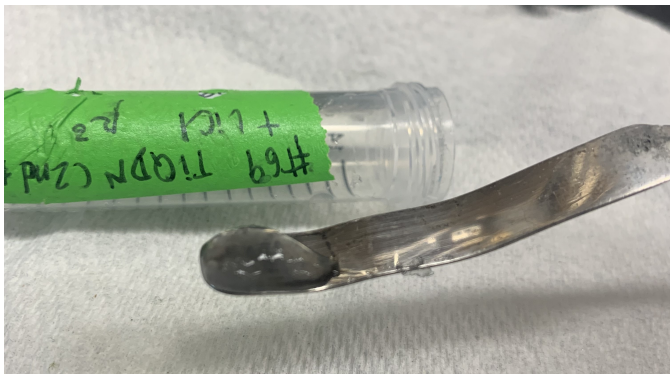
Figure E.1. Image of the TiC-based 1DL after lithium chloride washing, shown here on a metal spatula.

Figure E.2. Image of the TiC-based 1DL after lithium chloride washing, shown here in its reaction tube.
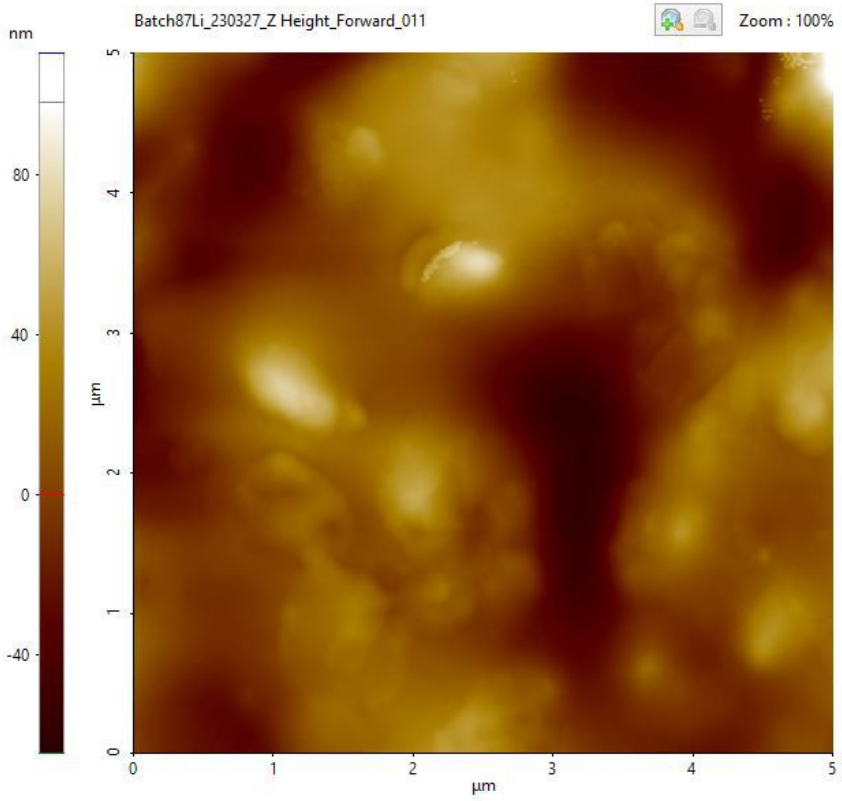
Figure E.3. AFM Image of Batch 87L1.